

Exceptional service in the national interest



Statistical Descriptions of Defect-Mediated Structure-Properties Relationships in Metals

Fadi Abdeljawad, Corbett Battaile, Joe Bishop, Brad Boyce, Luke Brewer, Jay Carroll, Blythe Clark, John Emery, Rich Field, Jay Foulk, Hojun Lim, Jon Madison, Steve Owen

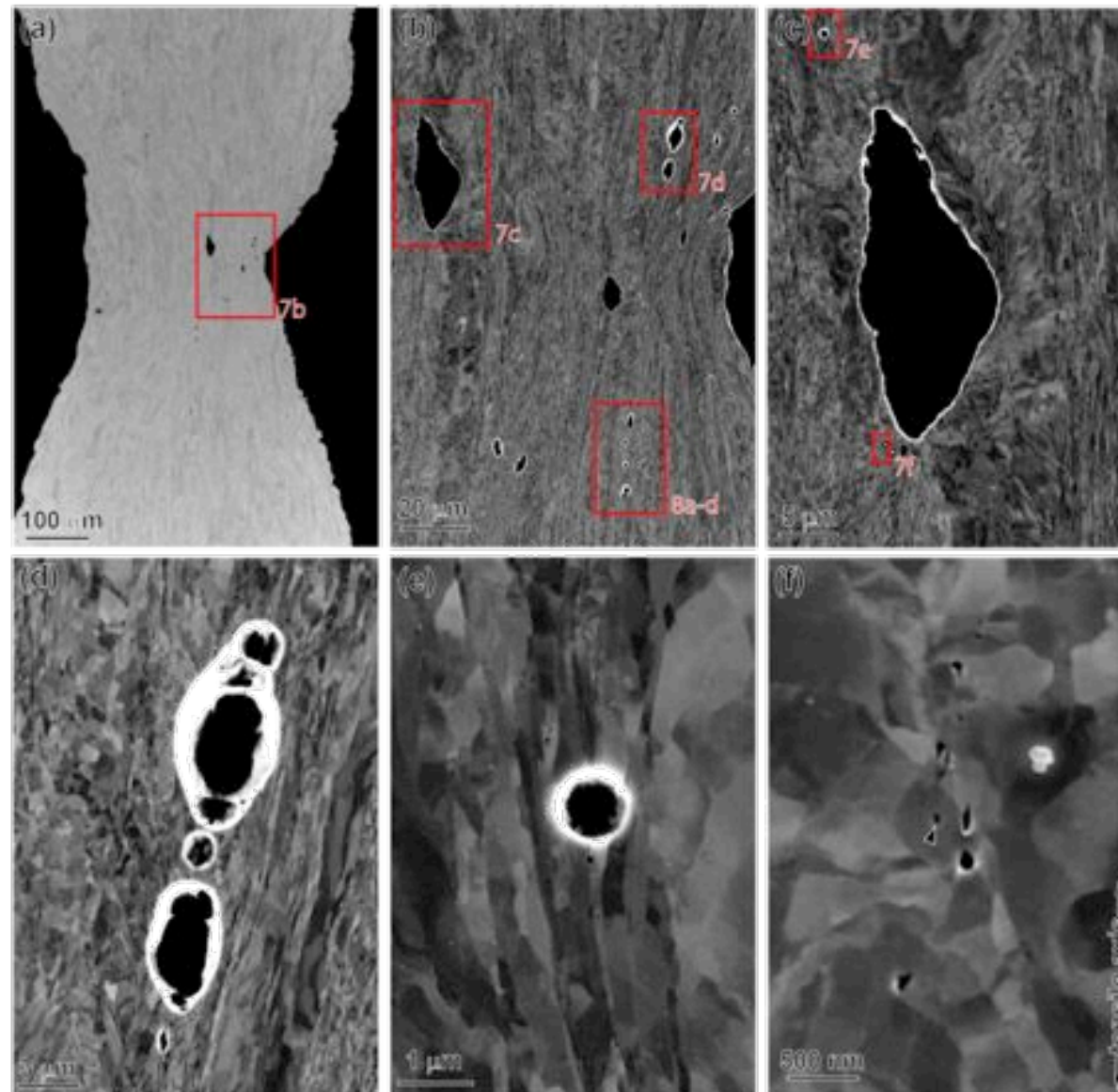
- In your Slide Master option, you have 5 other title pages to choose from based on your content information. If you need help with this presentation or would like added material call the Creative Group at 844-6416.
- Thank you

Outline

- Characterization of voids in deformed Ta and welded 304L stainless steel
- Simulations of microstructure-induced uncertainty in metal deformation near defects
 - Holes in brass
 - Notches in Ta
 - Micro-springs
- Direct numerical simulations of microstructure-scale mechanics in engineering-scale components
- Stochastic reduced-order models for mechanical properties of partial-penetration 304L laser welds
- Conformal, hexahedral finite element meshing technology for three-dimensional polycrystalline microstructures

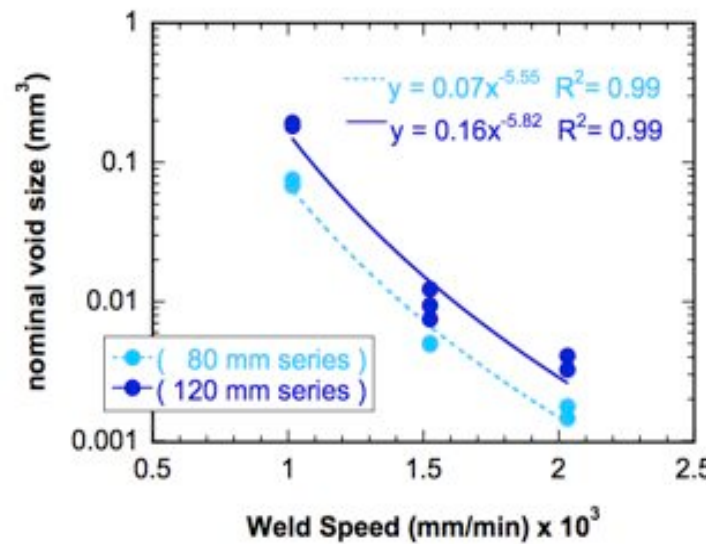
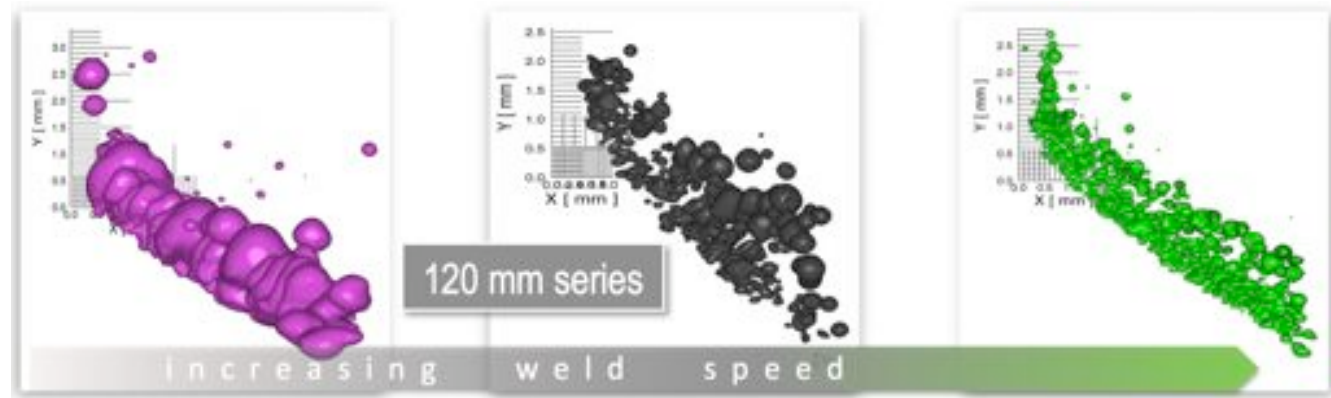
Characterization of voids in deformed Ta and welded 304L stainless steel

Voiding During Deformation (Ta)



Manufacturing Defects (304L Weld)

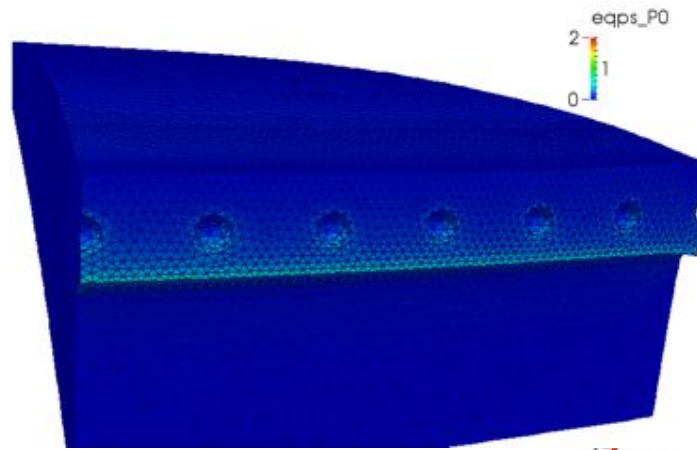
- CT data analyzed to determine porosity size and shape distributions as a function of weld speed.
- Porosity in 304L stainless steel welds was successfully observed and characterized for three weld speeds.



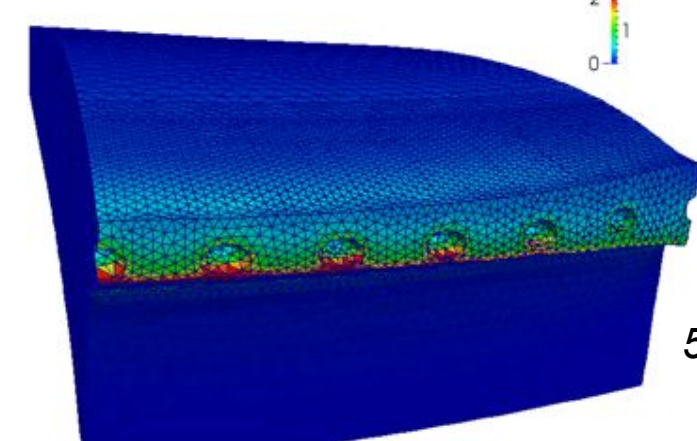
3D characterization of porosity will inform construction of model weld geometries for computational analysis and homogenization.

Pores imaged via microtomography can be fully characterized in 3D. Note substantial decrease in pore size as weld speed increases.

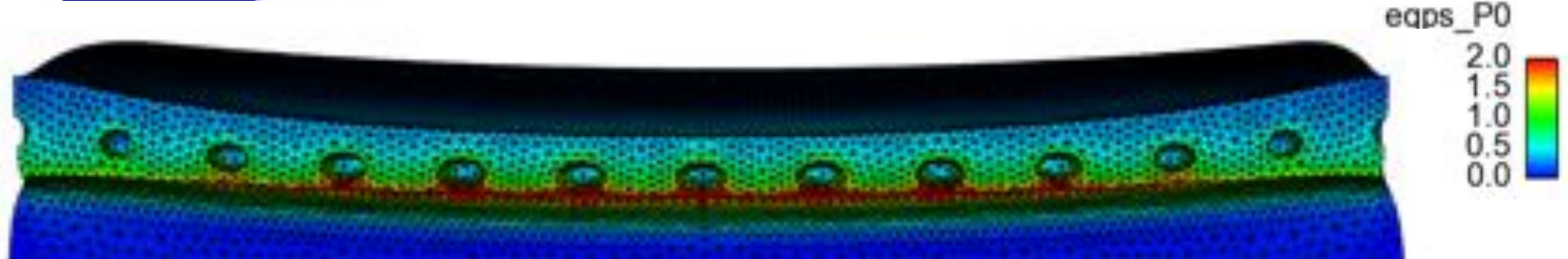
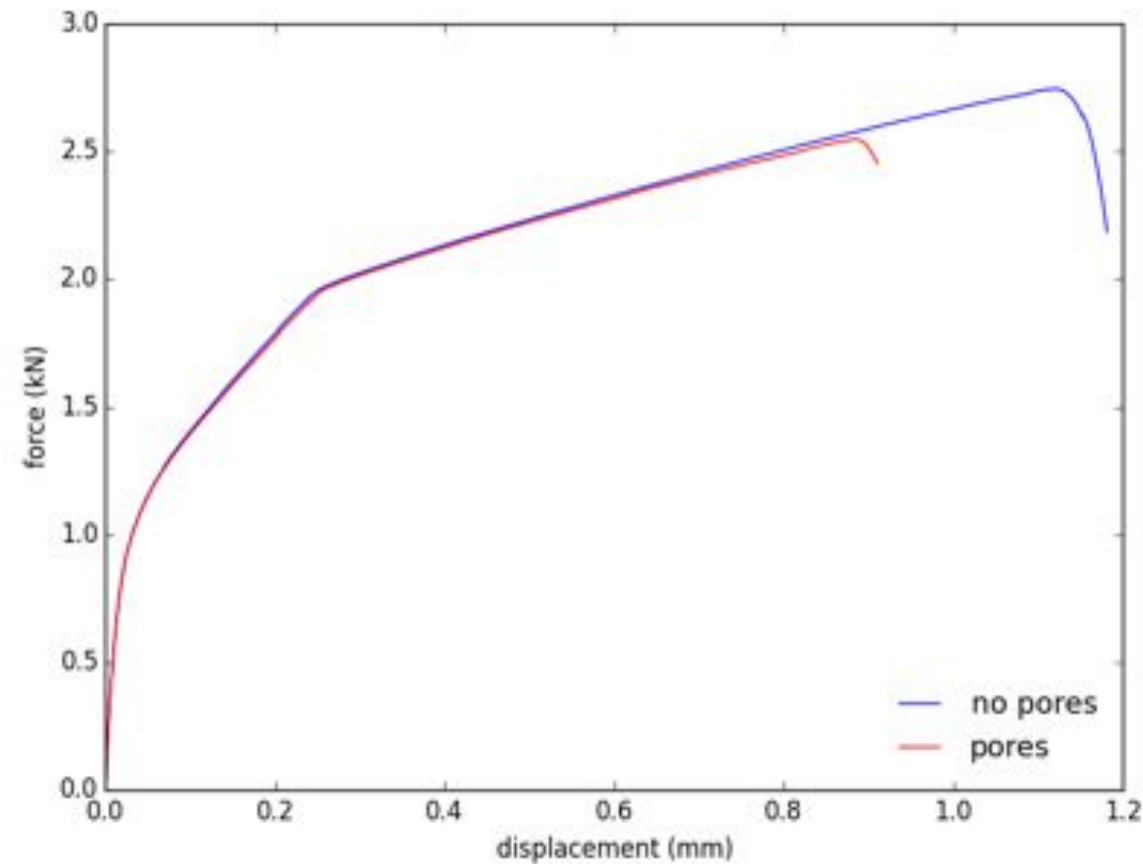
Effects of Porosity on Properties



1st map



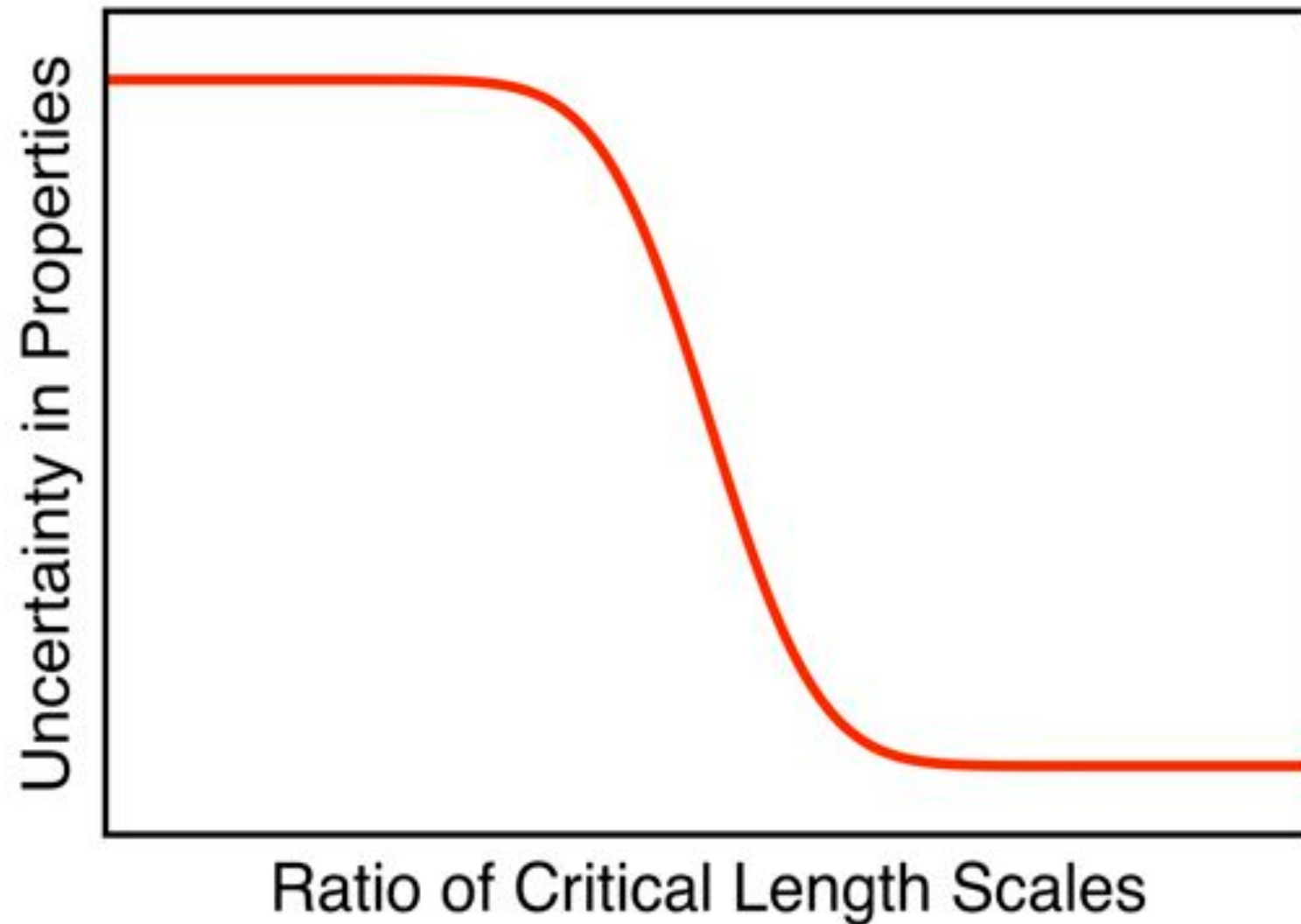
5th map



eqps_P0
2.0
1.5
1.0
0.5
0.0

Simulations of microstructure-induced uncertainty in metal deformation near defects

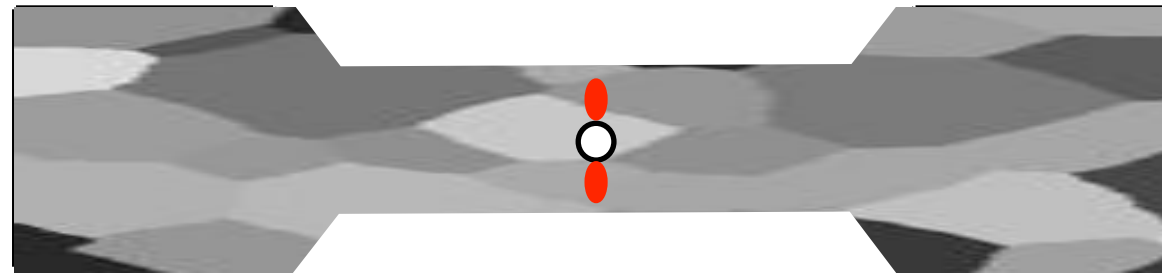
Uncertainty Depends on Scales



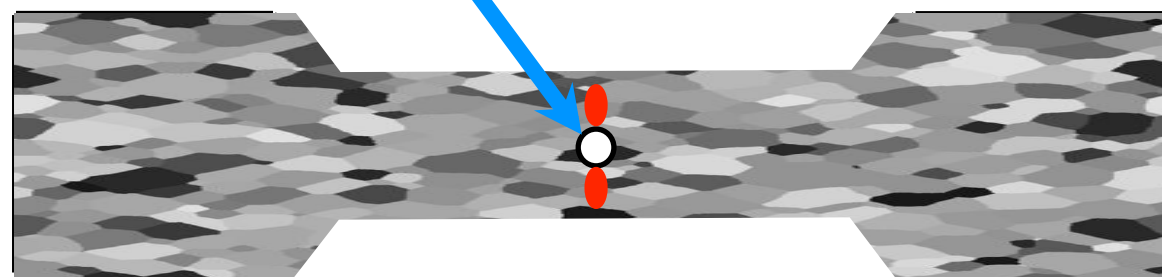
Tensile Experiments, Varying Scale

Localization of deformation near a small hole should interact directly with microstructure if the relevant scales are appropriate.

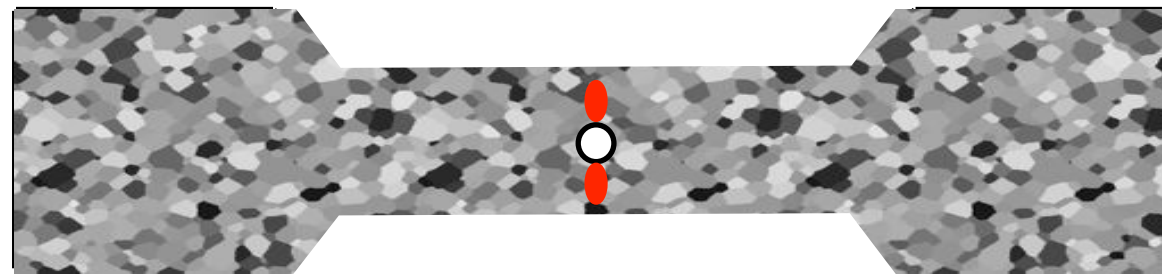
Hole \sim 100 μm diameter,
via femtosecond laser.



Coarse ($R < 1$)
8 hr, 800 °C
725.2 μm
62.7 MPa



Medium ($R = 1$)
8 hr, 600 °C
79.1 μm
91.7 MPa

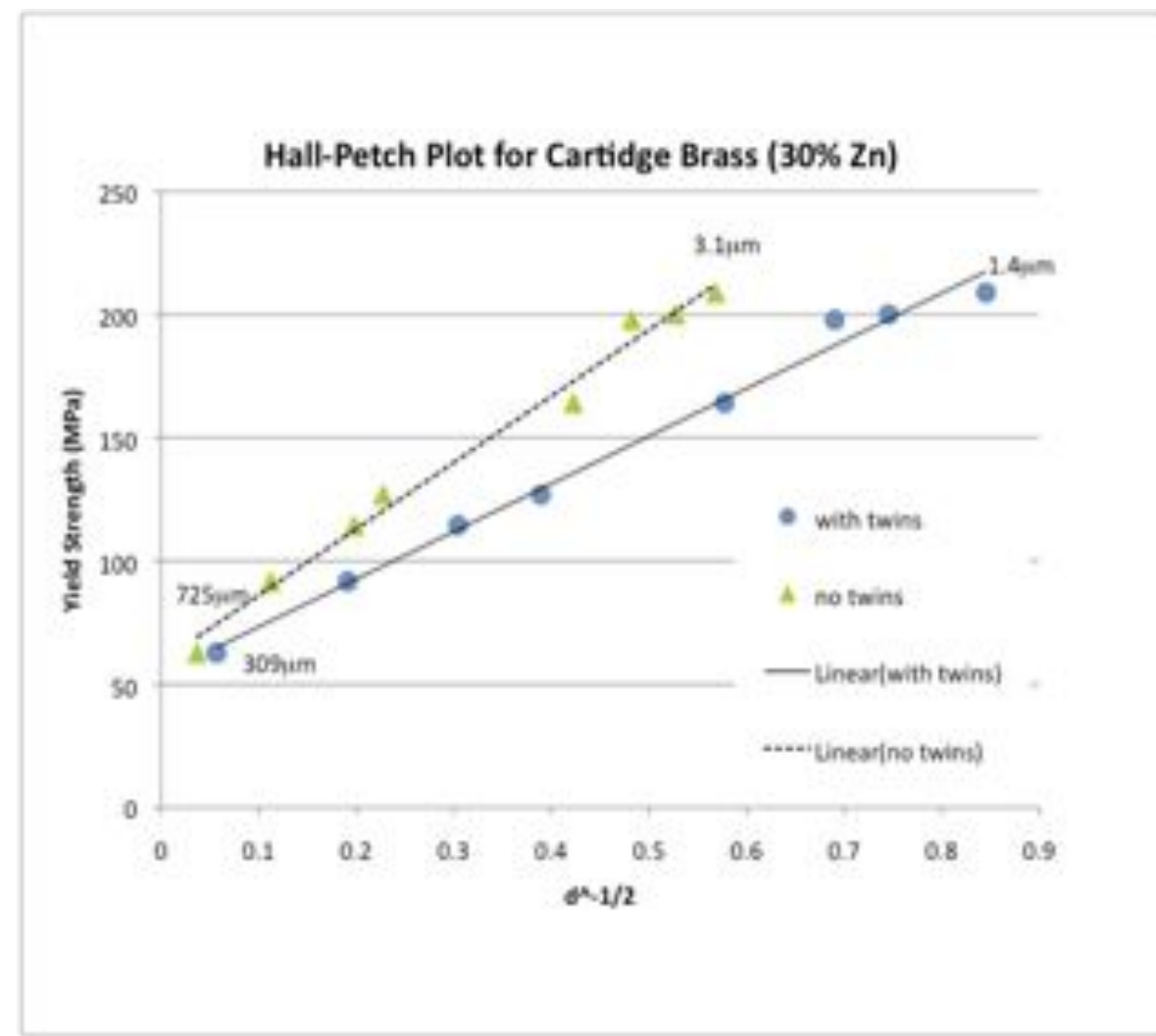
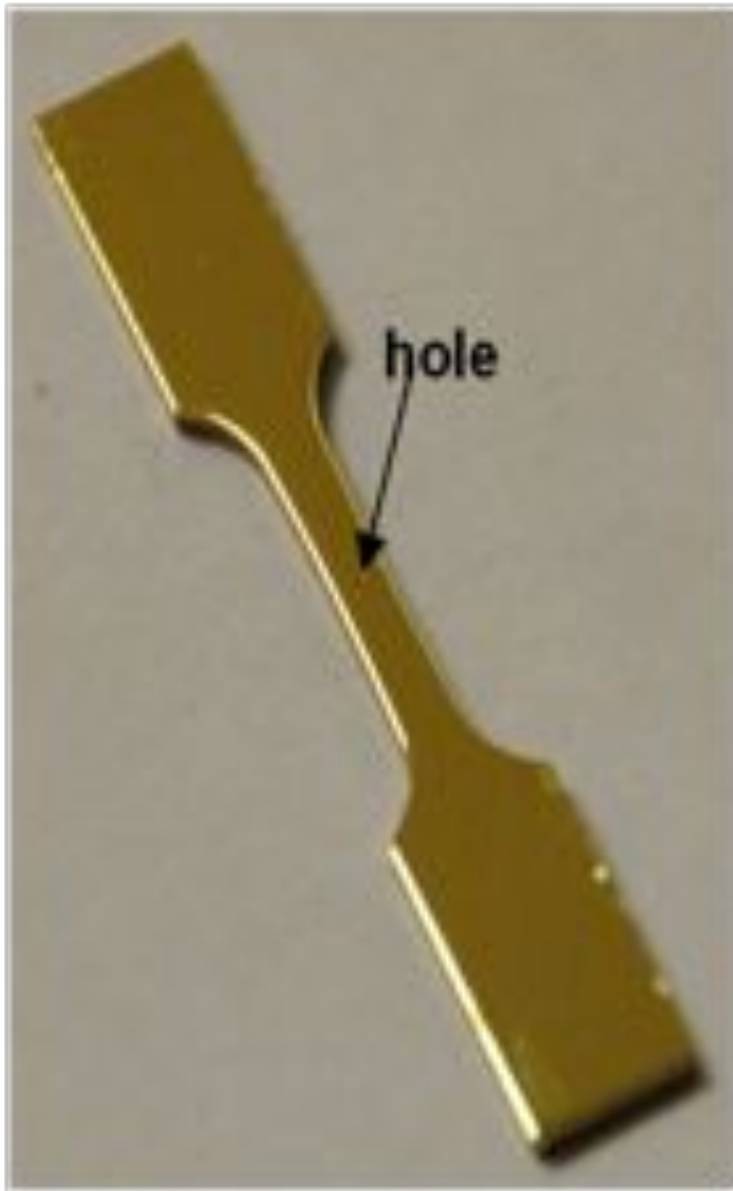


Fine ($R > 1$)
8hr 450°C
725.2 μm
62.7MPa

R is the ratio of HOLE SIZE to GRAIN SIZE.

Tensile Samples with Micro-Holes

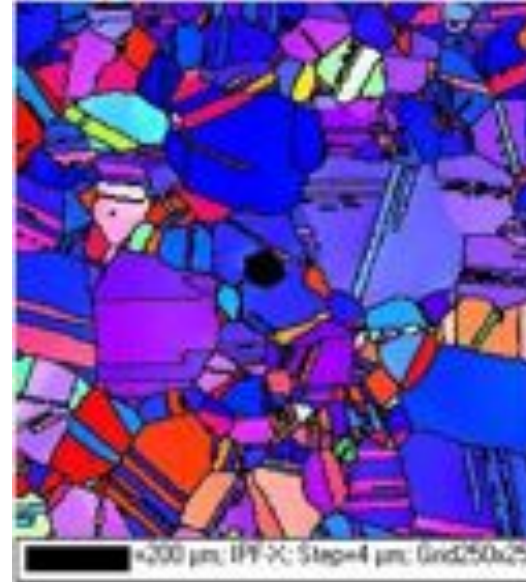
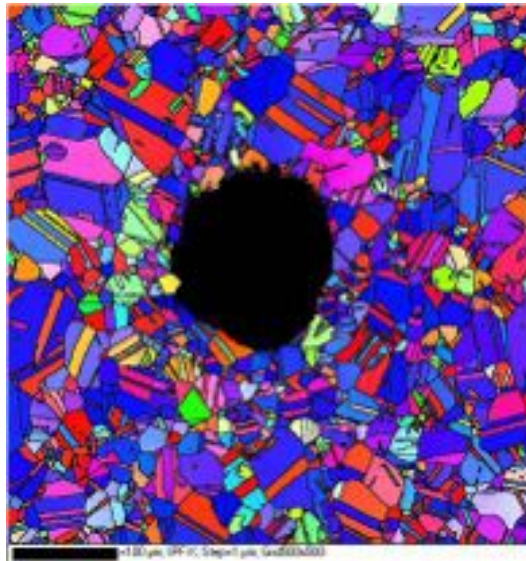
~ 100 μm holes “drilled” in brass specimens via femtosecond laser.



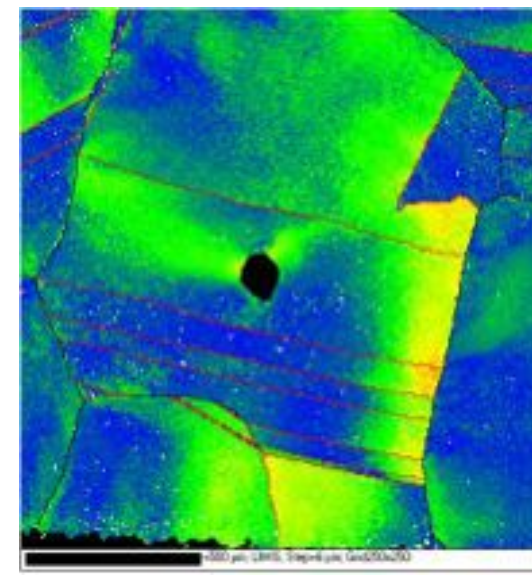
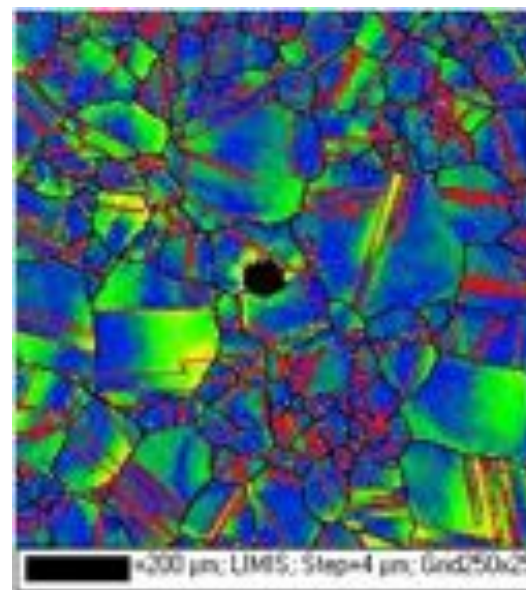
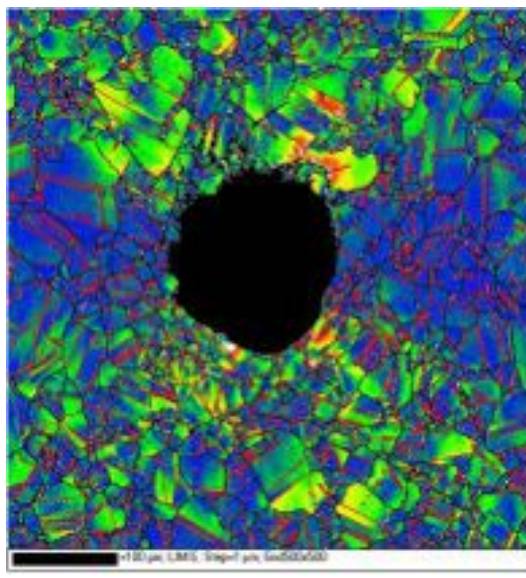
EBSD on Deformed Brass Samples

2% Applied Strain

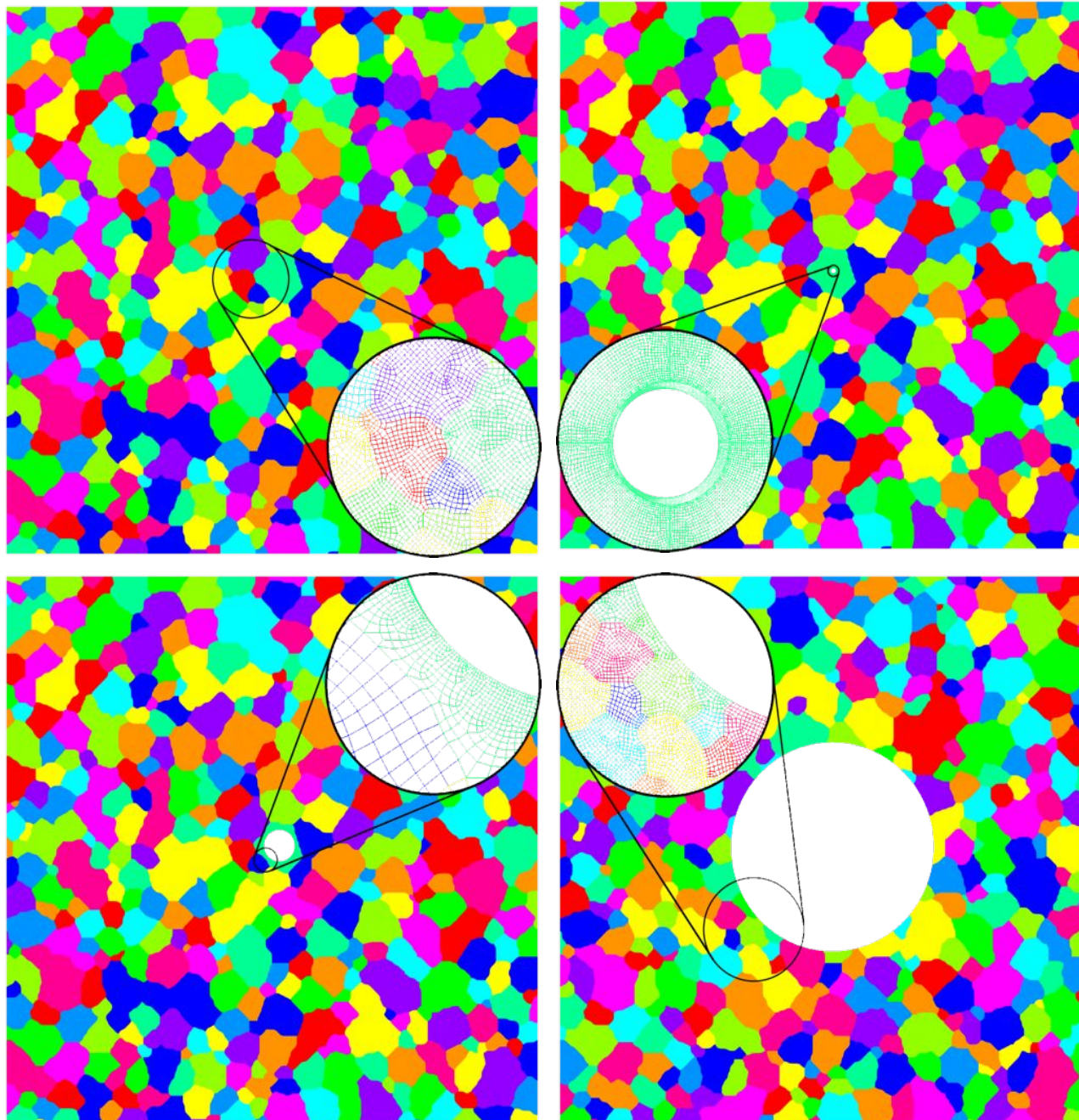
Inverse Pole Figure Maps
(tensile direction)



LIMIS Maps

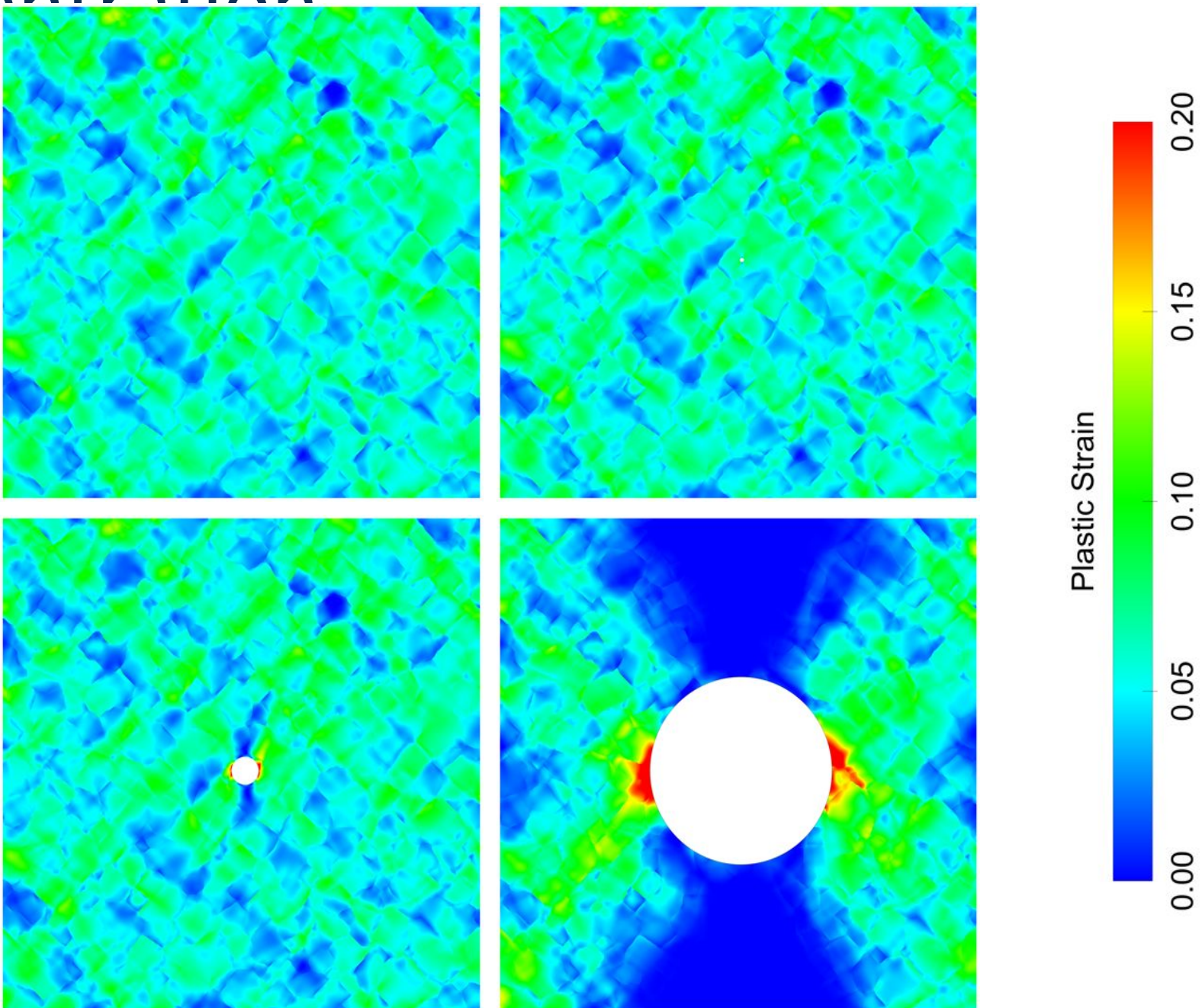


Finite Element Models



Simulated Plastic Strain Concentration

5% Applied Strain

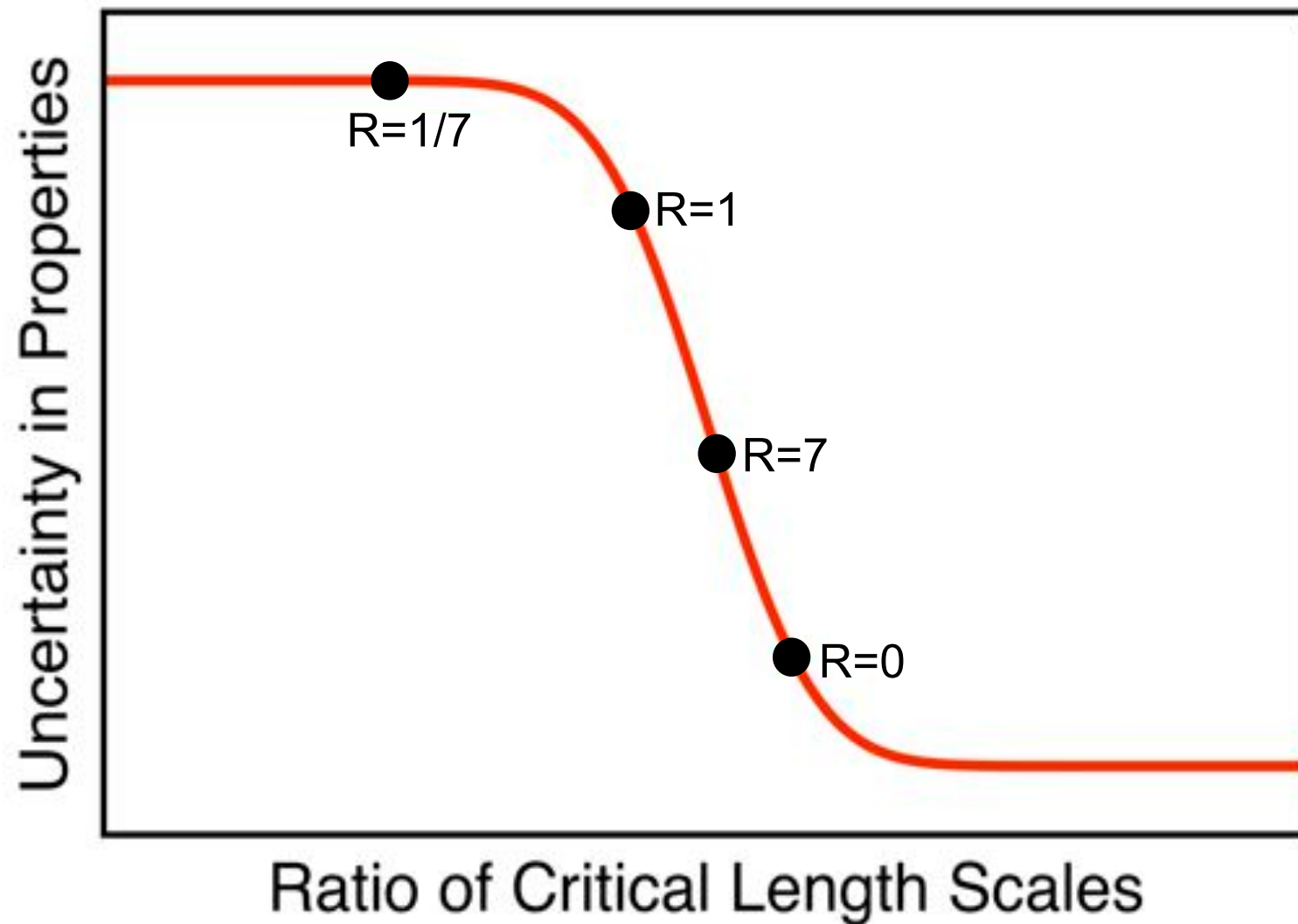


Variability in Strain Extrema

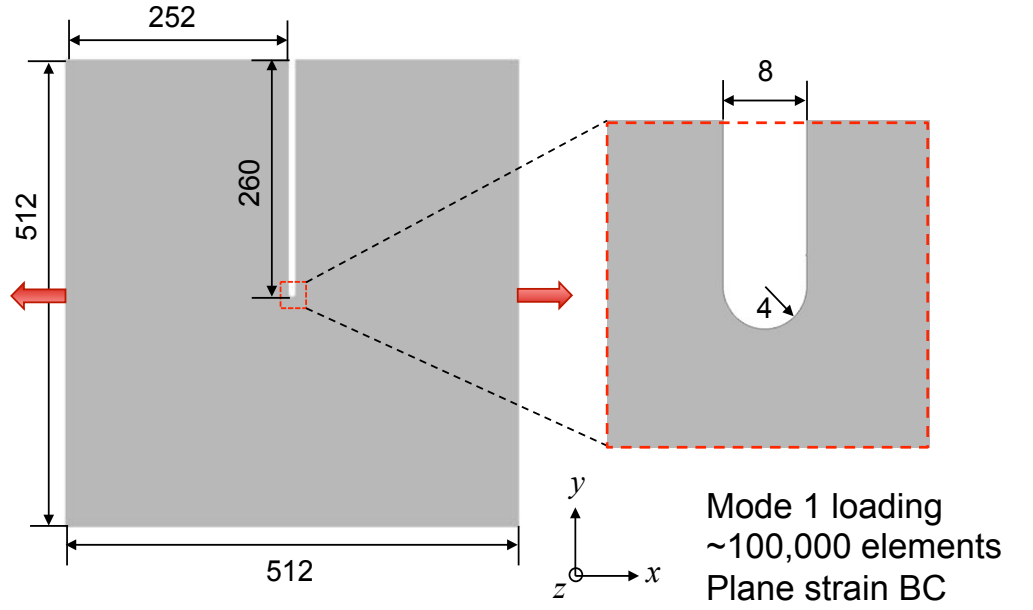
Moments of distributions of maximum plastic strain at 5% applied strain:

	R=0	R=7	R=1	R=1/7
N	45	45	45	45
μ	0.1631	0.3254	0.3194	0.2626
σ	0.0168	0.0440	0.0773	0.0972
σ/μ	10%	14%	24%	37%

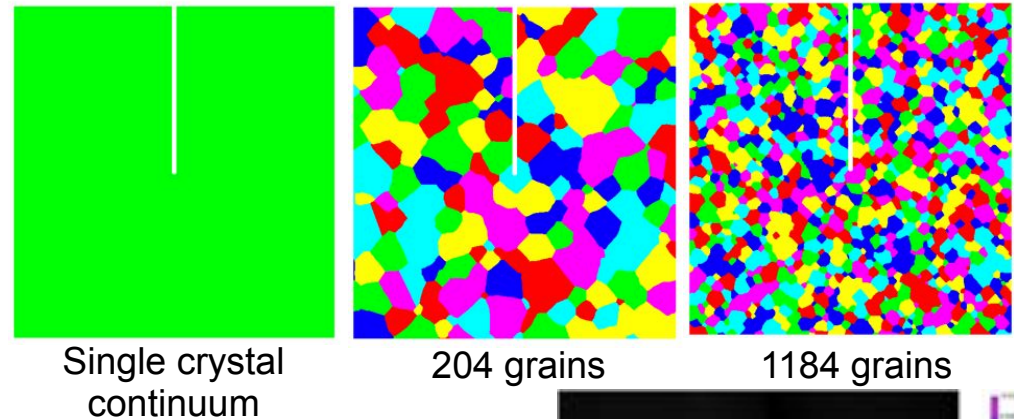
Uncertainty Depends on Scales



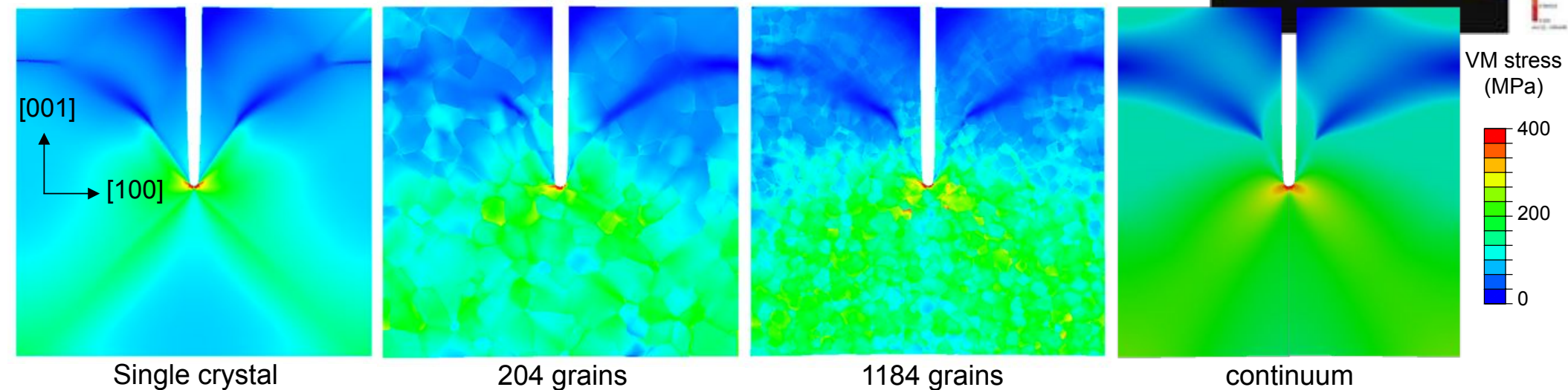
Simulations of Notched Ta



Initial microstructures

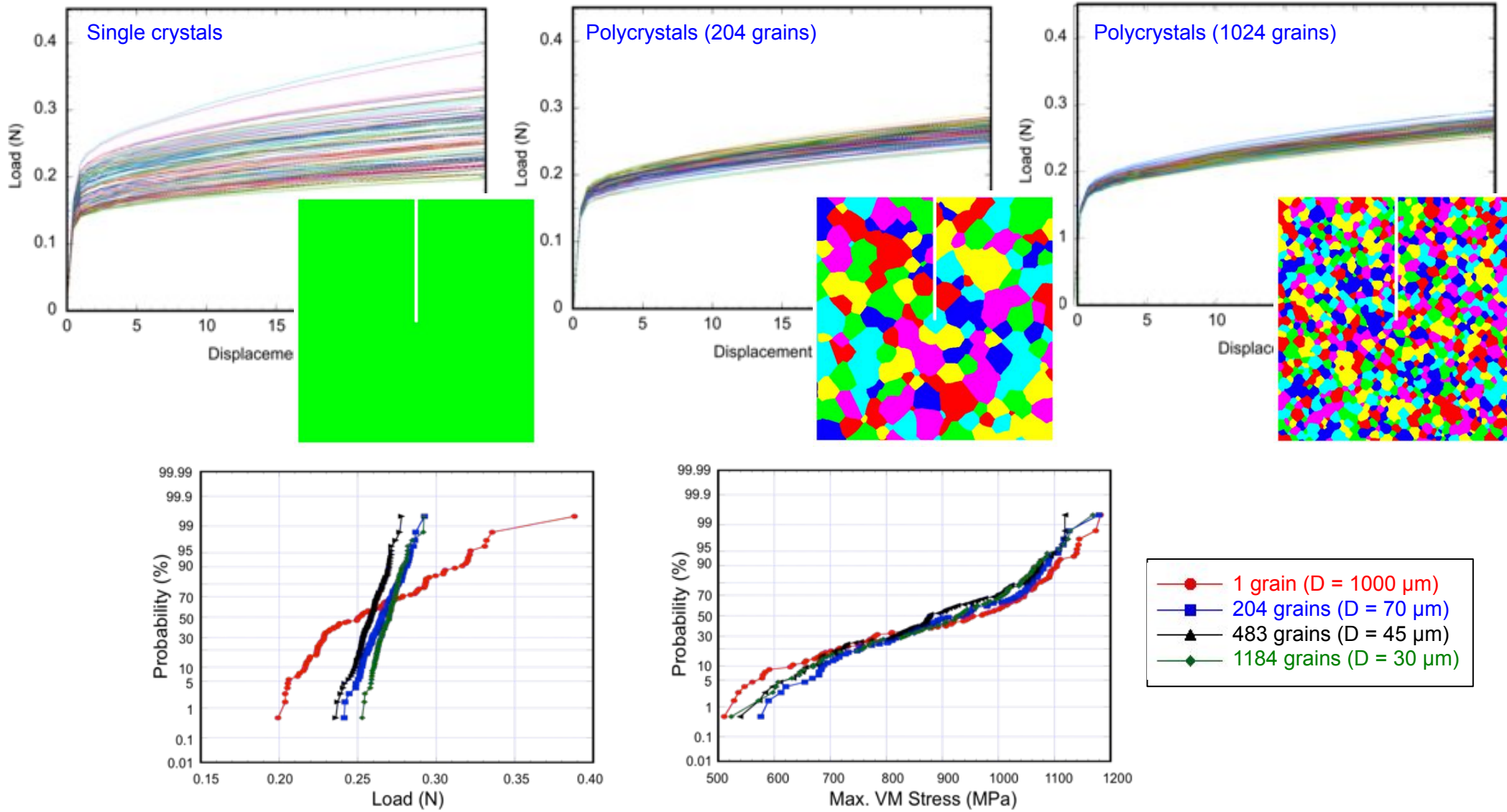


Von Mises stress predictions (applied strain = 3%)



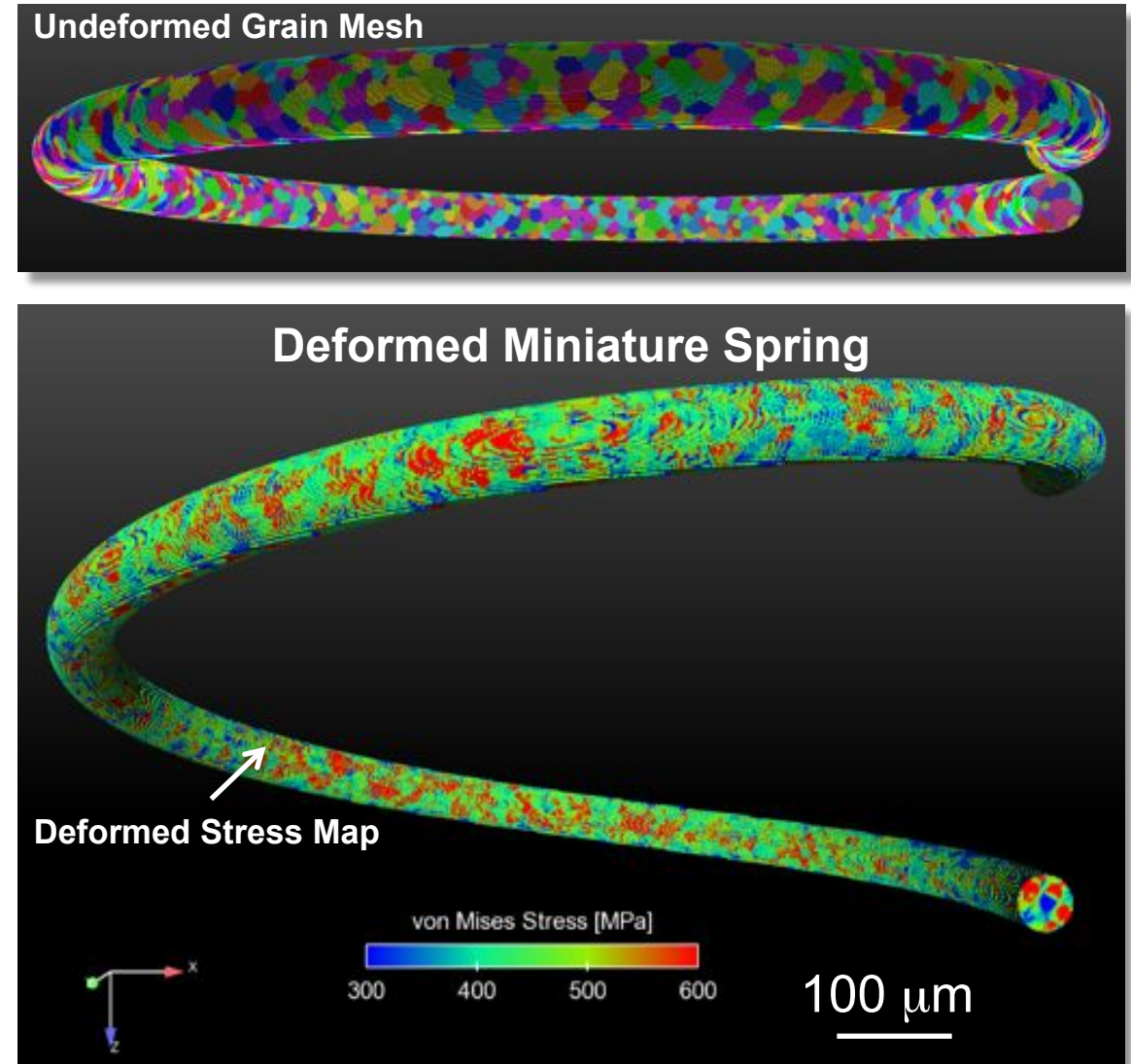
Simulations of Notched Ta

Connecting microstructural variability to stochastic performance



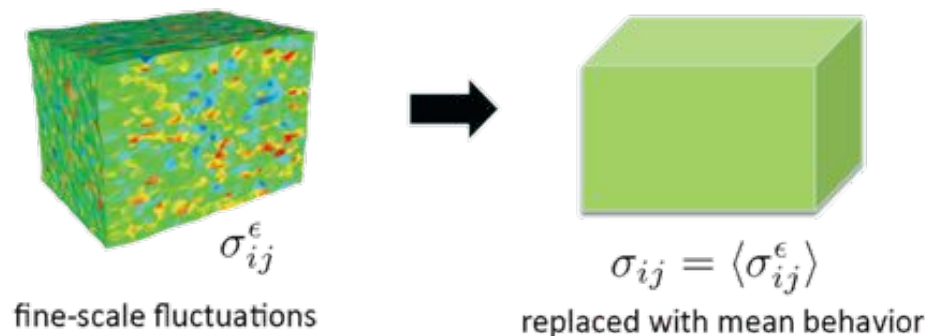
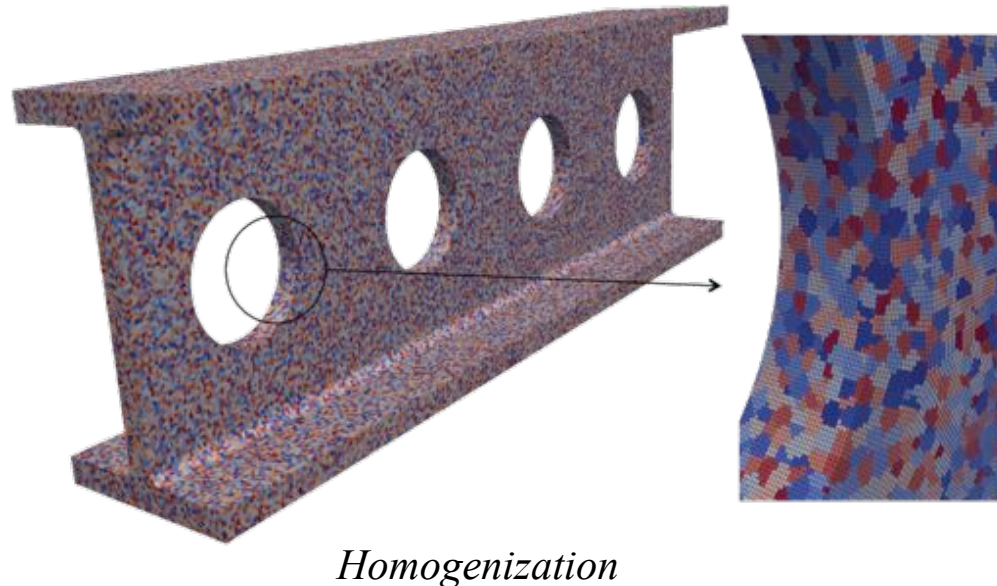
Variability in load-displacement and localized max. VM stress from 100 realizations

Microstructured Micro-Springs

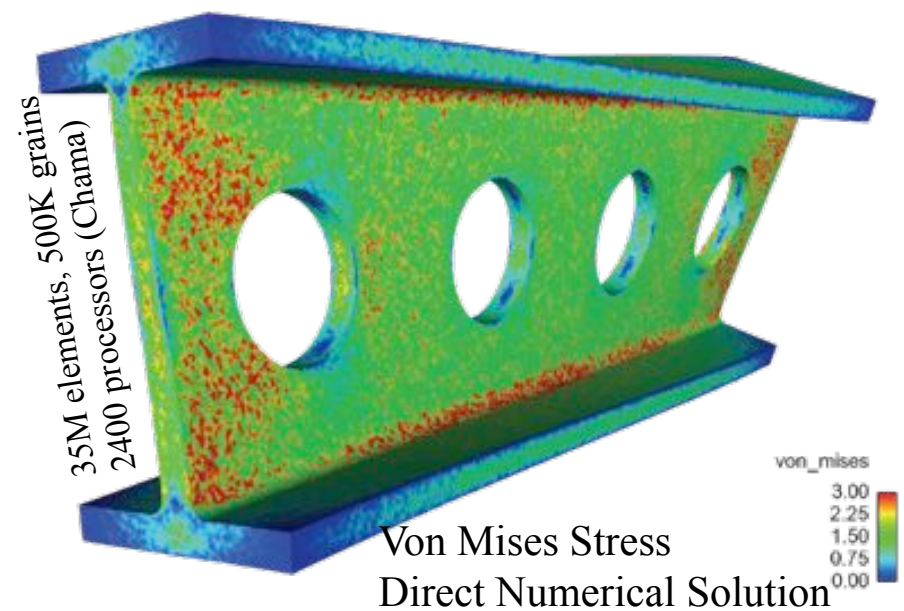


*Stress variations in a miniature
Inconel X750 spring microstructure.*

Direct Numerical Simulations: Beam

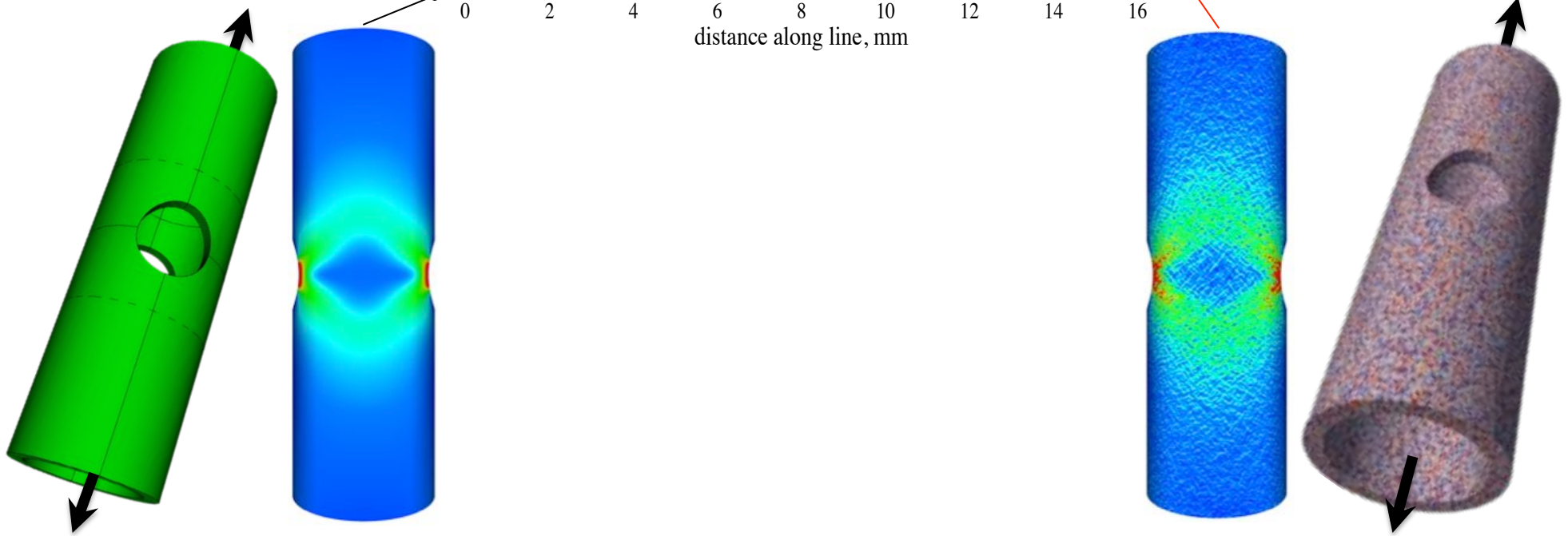
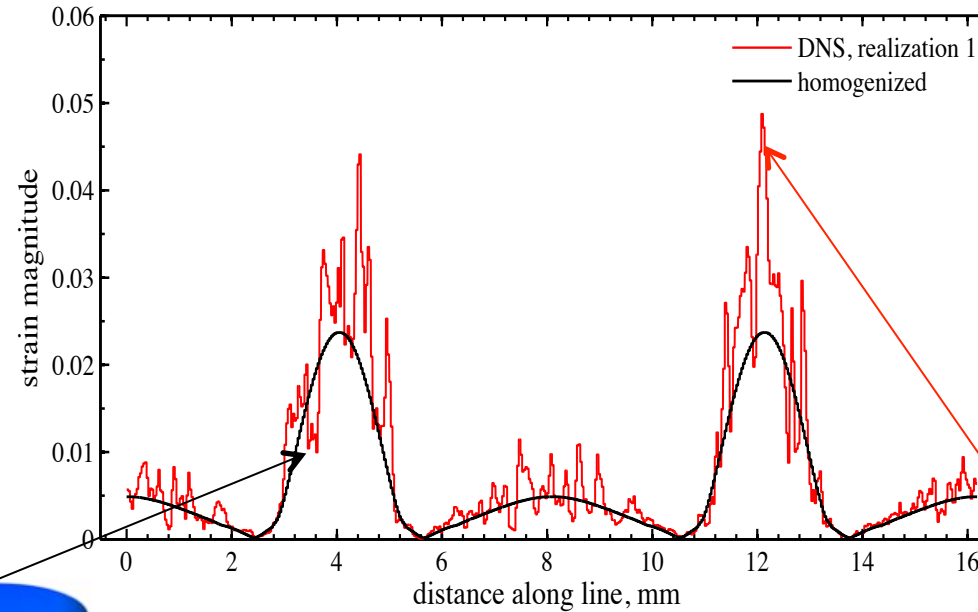


This equivalence is defined in an energy sense: $\sigma_{ij}\varepsilon_{ij} = \langle \sigma_{ij}^{\epsilon} \rangle \langle \varepsilon_{ij}^{\epsilon} \rangle$



Direct Numerical Simulations: Tube

Comparison of strain field around side-hole

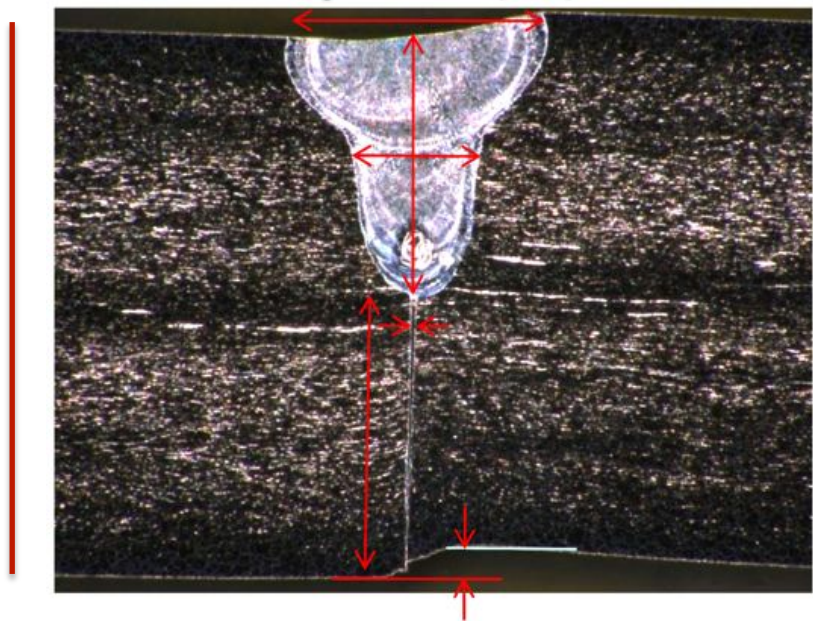
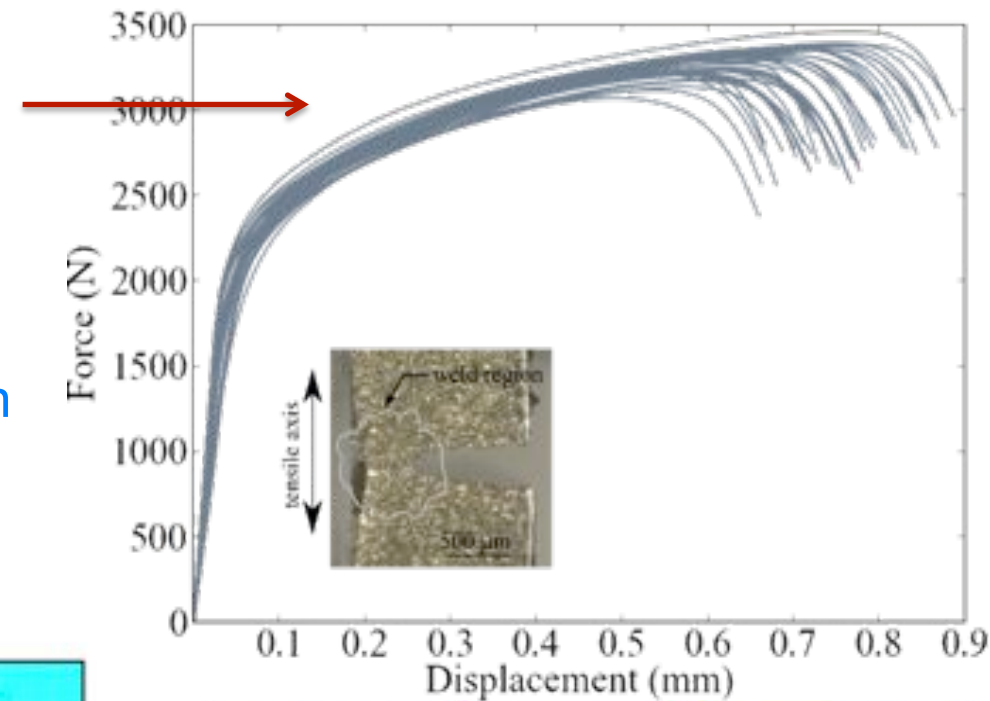
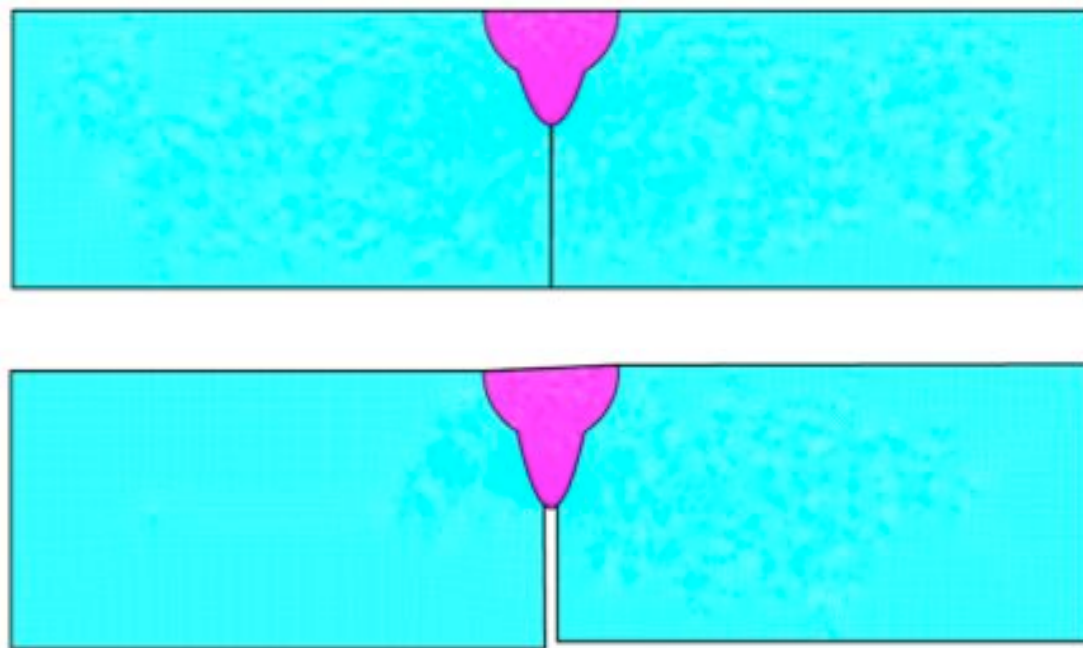


Stochastic reduced-order models for mechanical properties of partial-penetration 304L laser welds

Variability in Weld Response

Forty (nominally) identical welded specimens show significant variability, particularly in localization and failure.

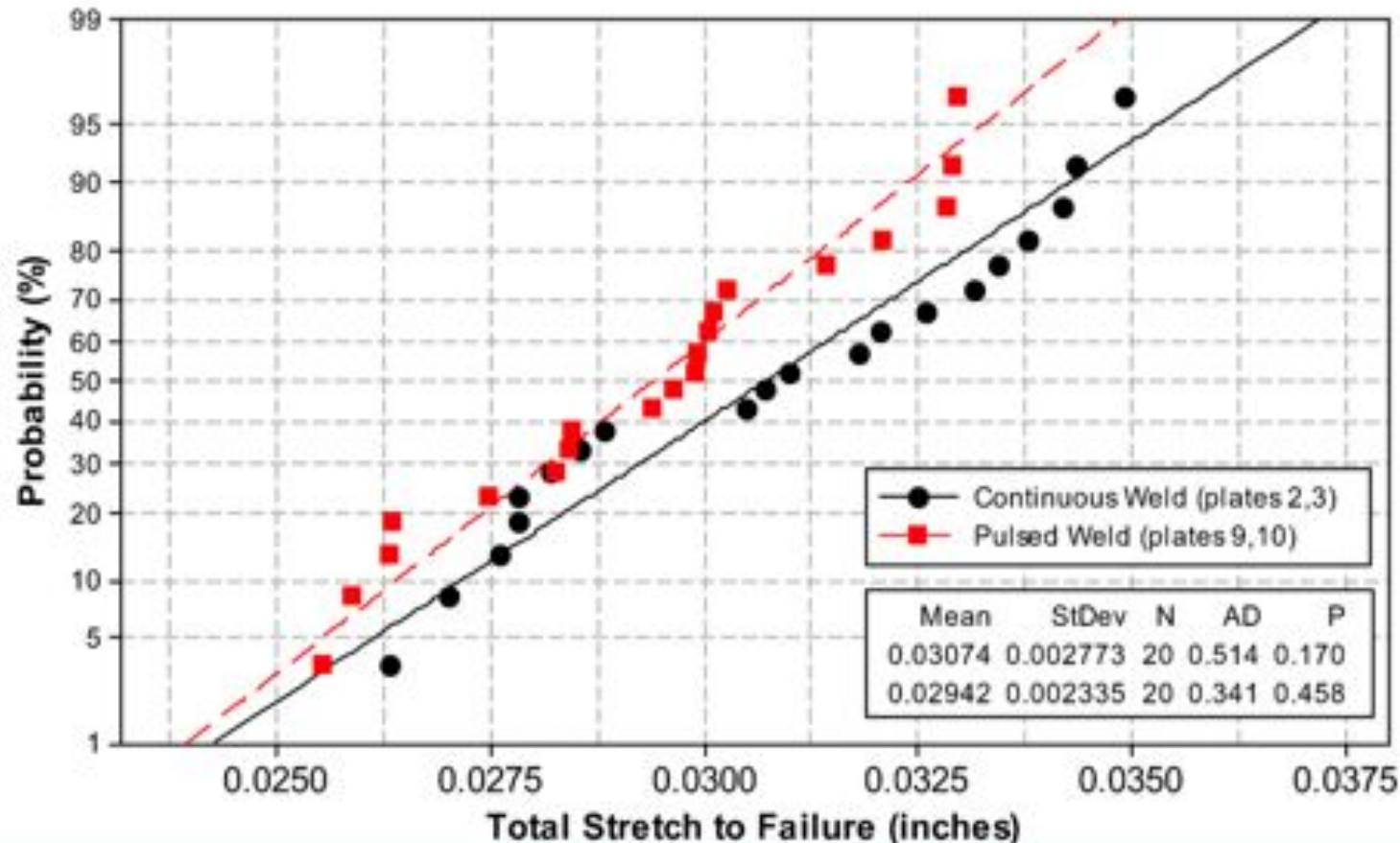
Simulated weld geometries attempt to capture realistic weld shape, in addition to variability in weld **depth**, **plate gap**, and **plate offset**.



Weld Variability Impacts Design

Among 15 common distributions, the Gaussian distribution provided the best fit to the stretch data based on the Anderson-Darling goodness-of-fit metric.

Gaussian Analysis of Stretch-to-Failure



Extrapolating 'continuous weld' distribution to a low allowable stretch:

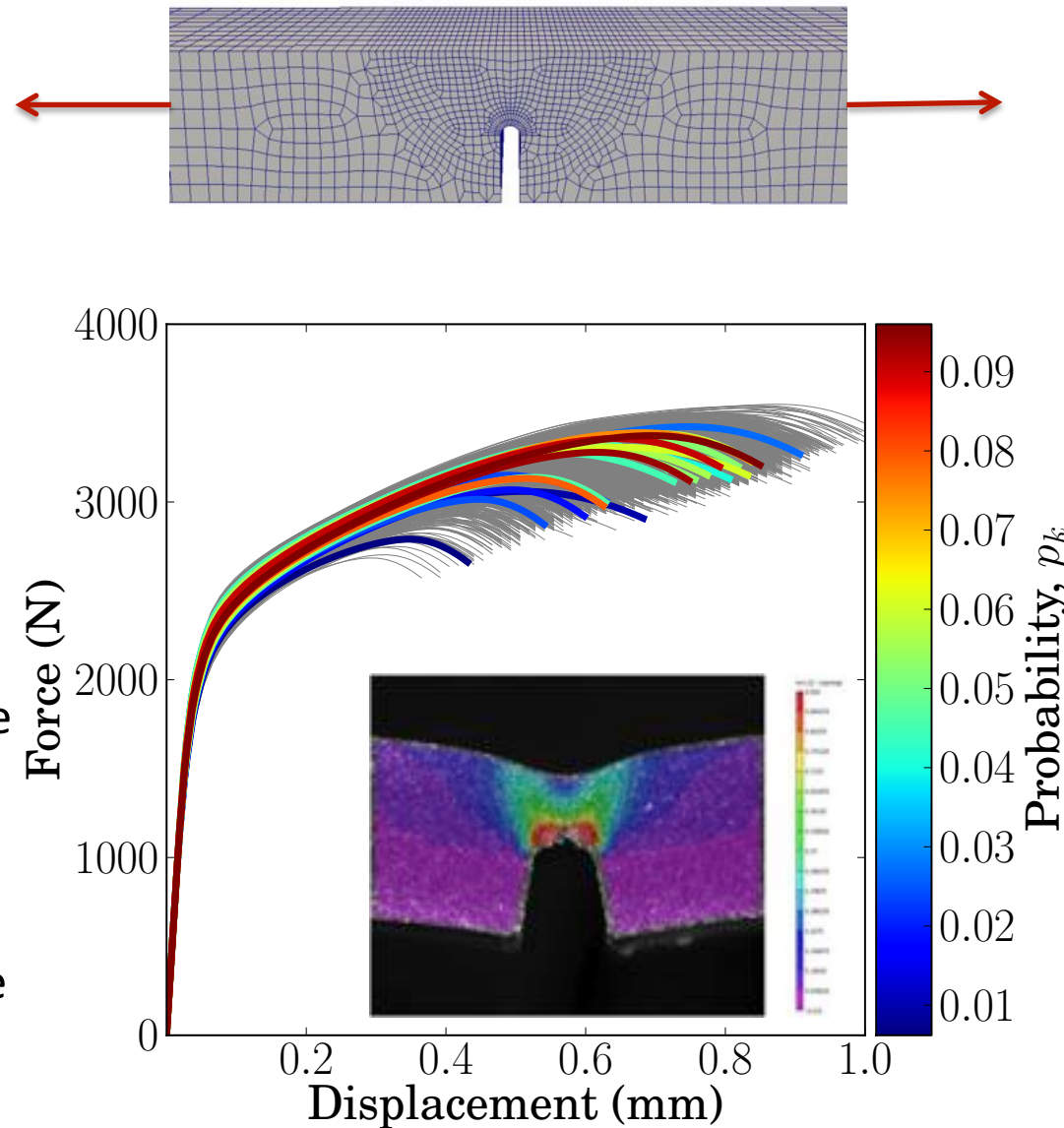
1-in-1,000 Allowable Stretch in Weld: 22.2 mils

1-in-1,000,000 Allowable Stretch in Weld: 17.6 mils

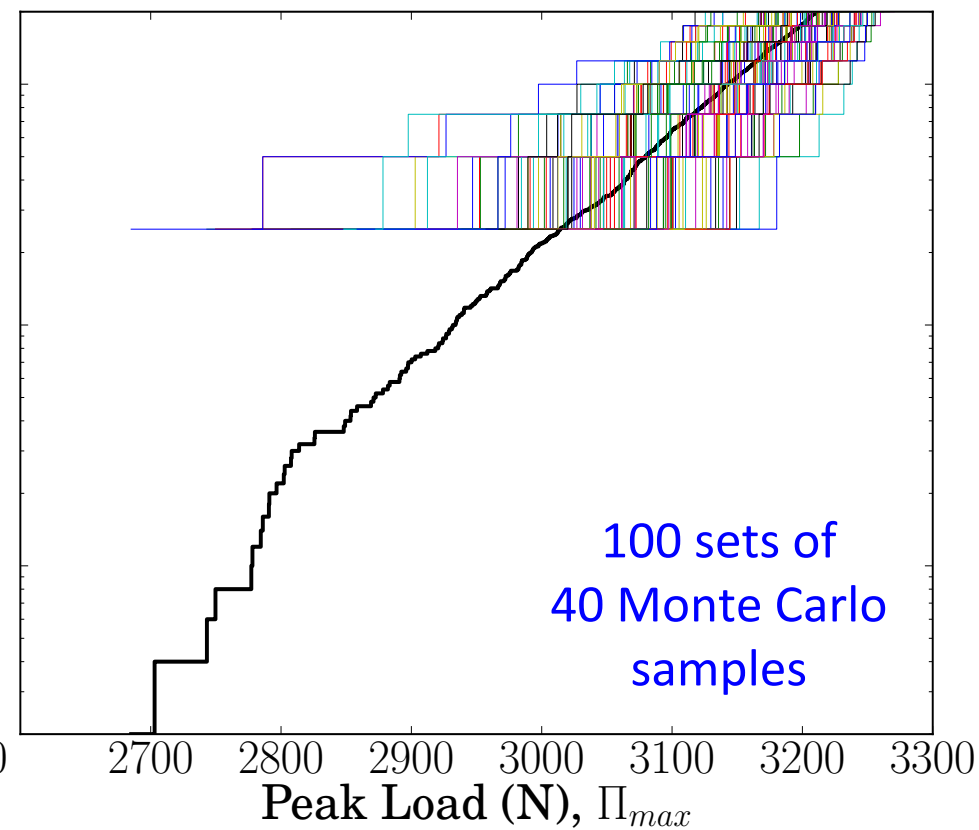
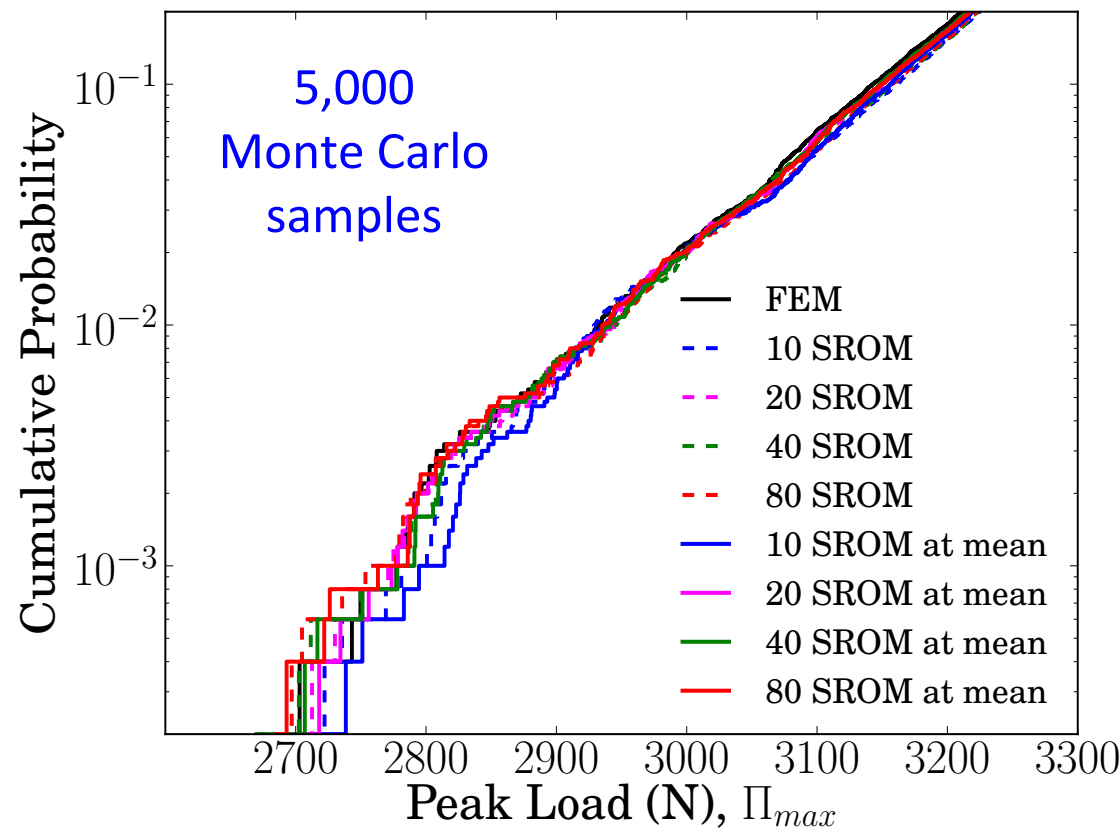
⇒ **Weld must be de-rated 43% below its average stretch for 1-in-1,000,000 Failure**

Stochastic Reduced-Order Model

- For verification, perform Monte Carlo simulation for the response of the laser welded tensile coupon.
- Generate 5,000 samples of Θ , do FE calculations – “Brute Force MCS”.
- Compare to the SROM-based surrogate (top) – “Smart MCS”.
- The 10 sample SROM-based surrogate model requires 40 FE calculations to construct (10 for each sample, 30 for the gradients).
- The CDF on the bottom was constructed with 100 sets of 40 FE calculations, no surrogate. It shows the wide confidence and large error...

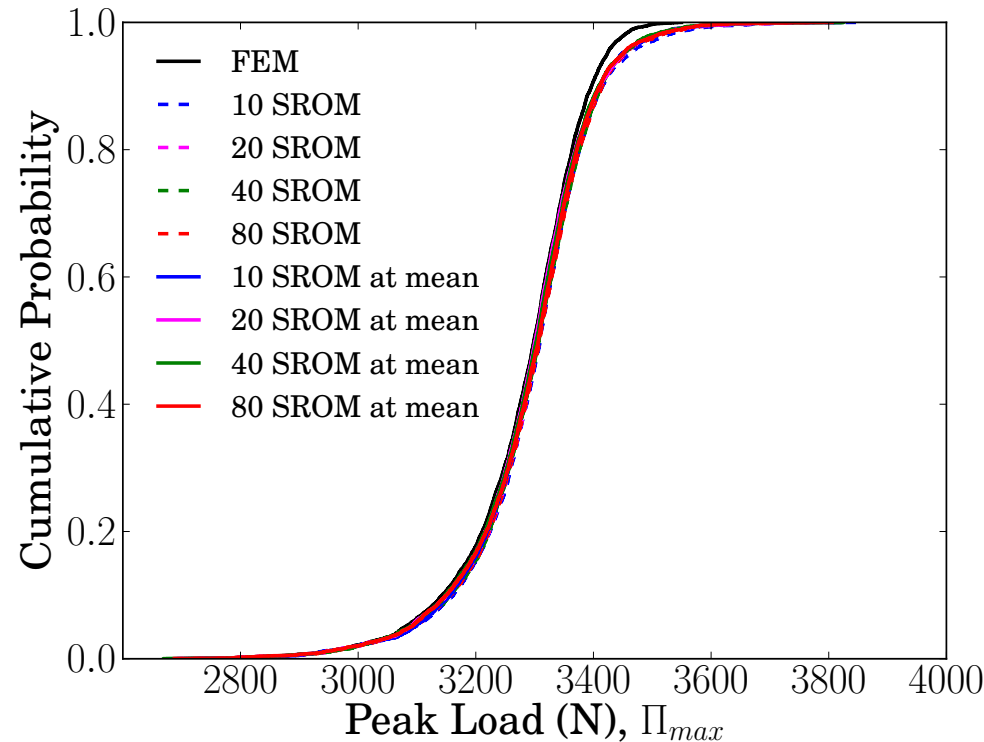


SROM versus “Brute Force”



SROM versus “Brute Force”

- SROM-based surrogate models replace component level FE models expediting Monte Carlo simulation while providing comparable accuracy.
- In practice, component level FE models cannot be run thousands of times. The SROM-based surrogate can.
- CPU time results are for the example shown here and compared with 5,000 FE calculations.



Computational expense in CPU seconds.

	Construct SROM*	FE calculations **	Evaluate surrogate*	Total
Brute force MCS	n.a.	33,400,000 (5,000 FE calculations)	n.a.	33,400,000
10 SROM at mean	948	511,000 (40 FE calculations)	6.69	512,000

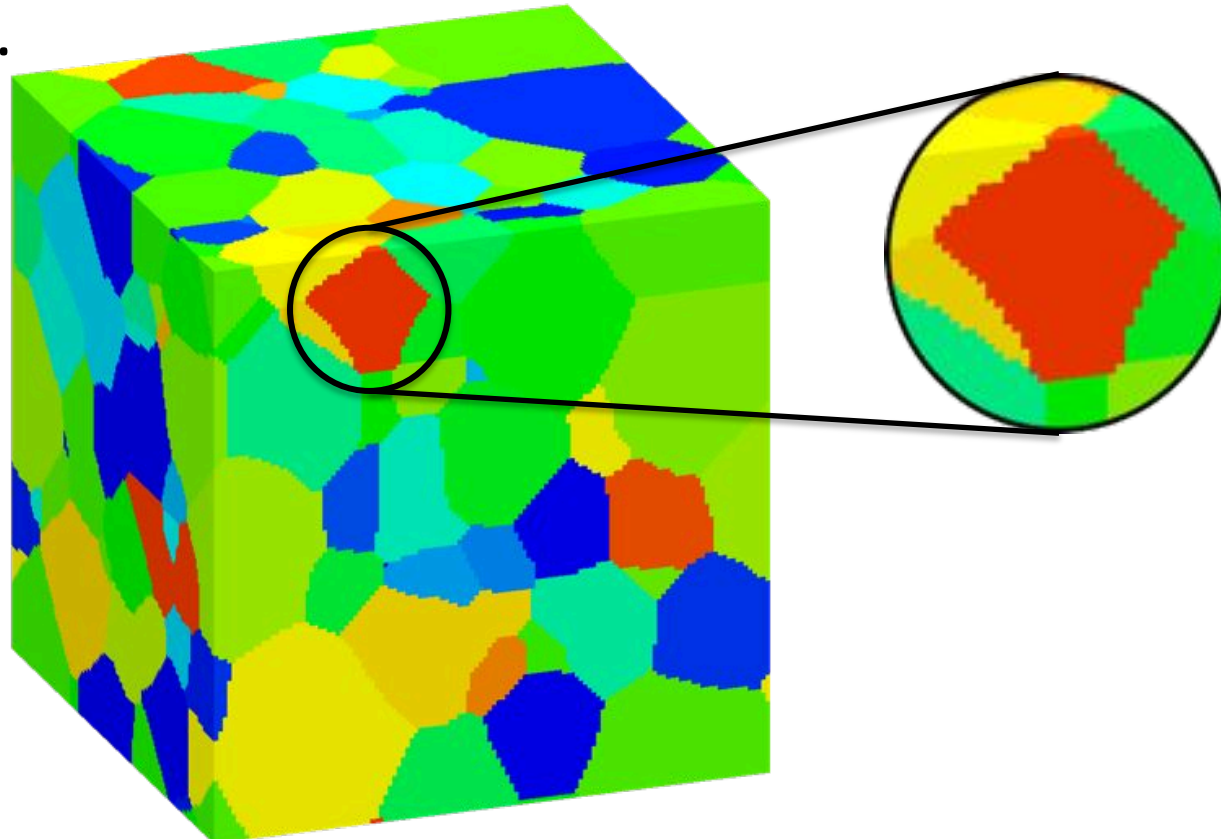
* Intel ® Xeon ® x5675 CPU @ 3.07 GHz w/ 48GiB RAM

** Intel ® Nehalem ® x5570 CPU @ 2.93 GHz w/ 1.5GiB RAM

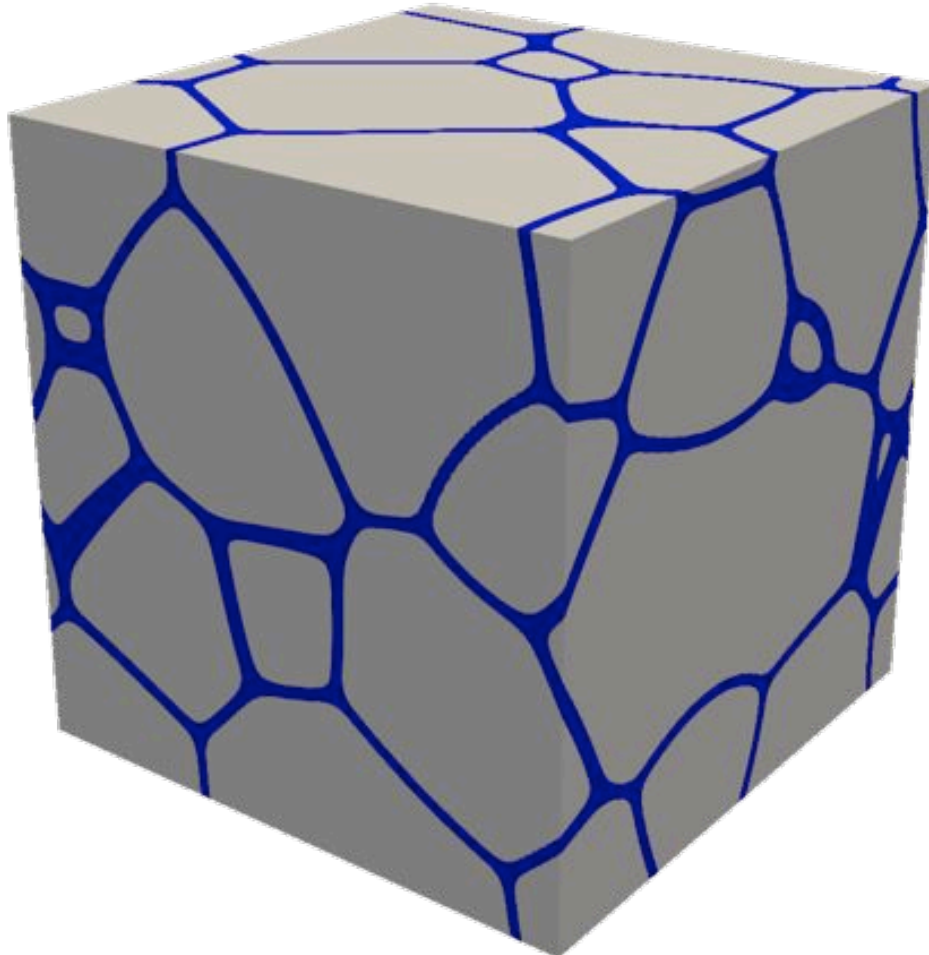
Conformal, hexahedral finite element meshing technology for three-dimensional polycrystalline microstructures

Why do we need mesh technology?

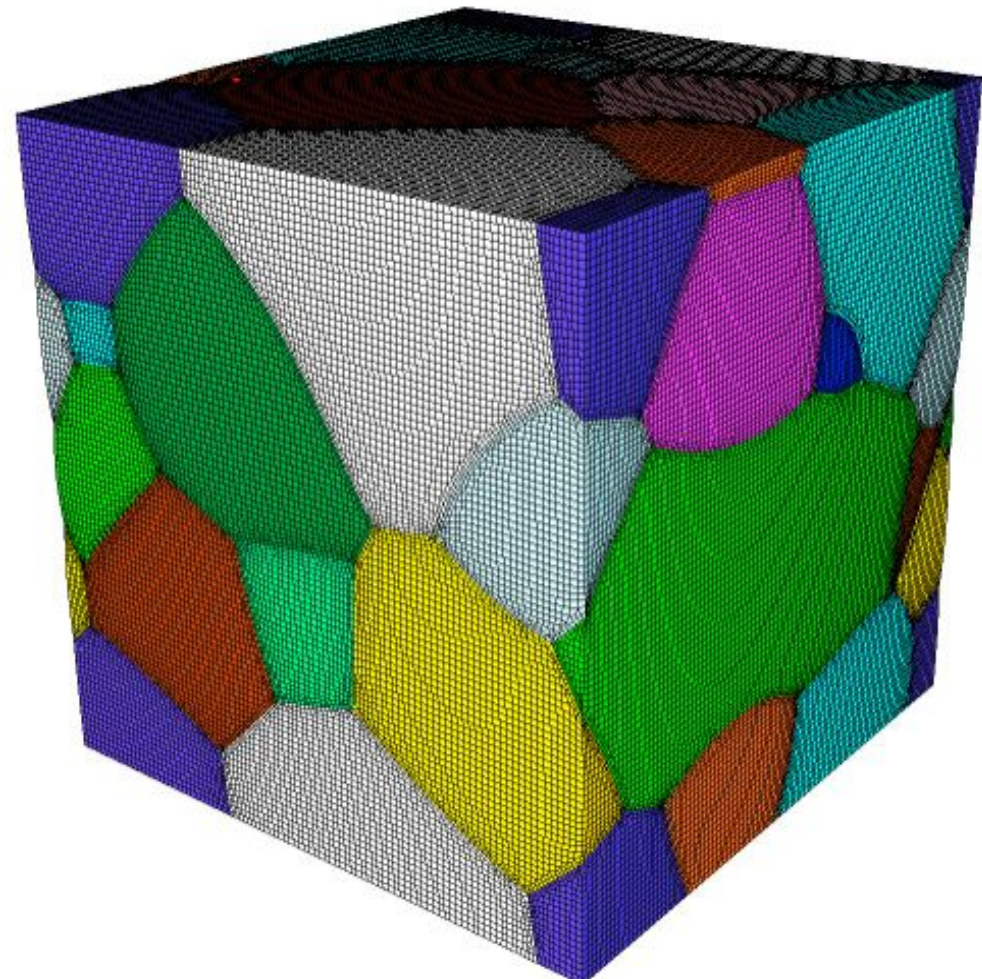
- Measured (EBSD) and synthetic (Monte Carlo, Phase Field) grain structures are represented on a grid.
- We usually map this grid directly onto finite elements of the same topology.
- This introduced artifacts (“jaggies,” “wedding cake”) at grain boundaries.



How can we better model GBs?

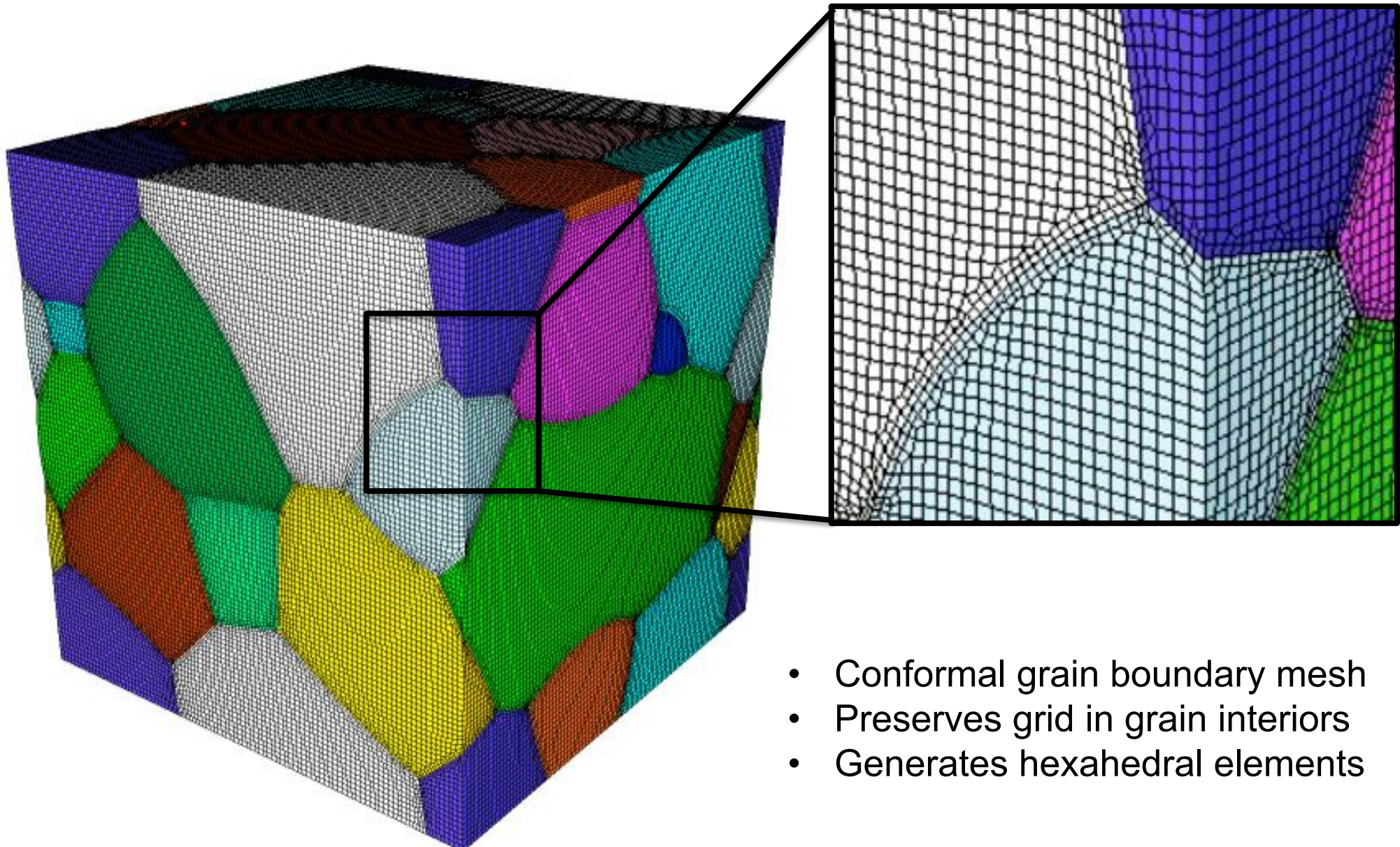


Phase Field Grain Growth Result



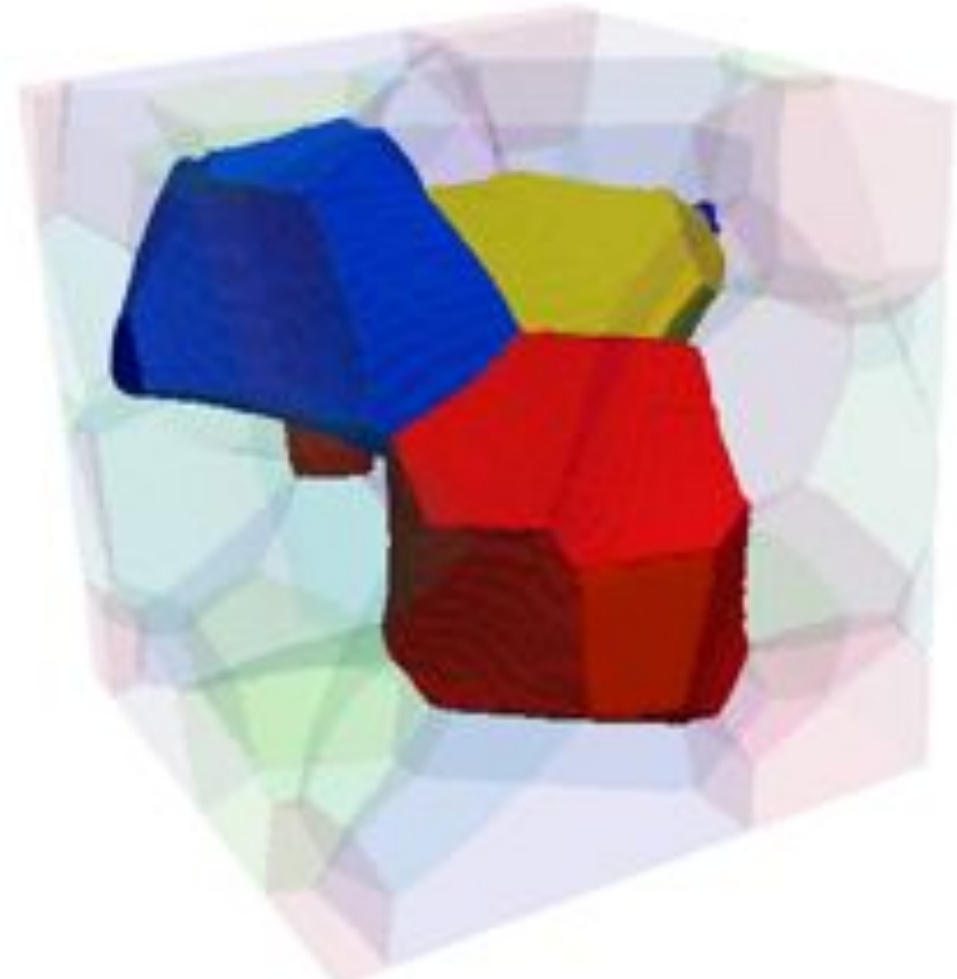
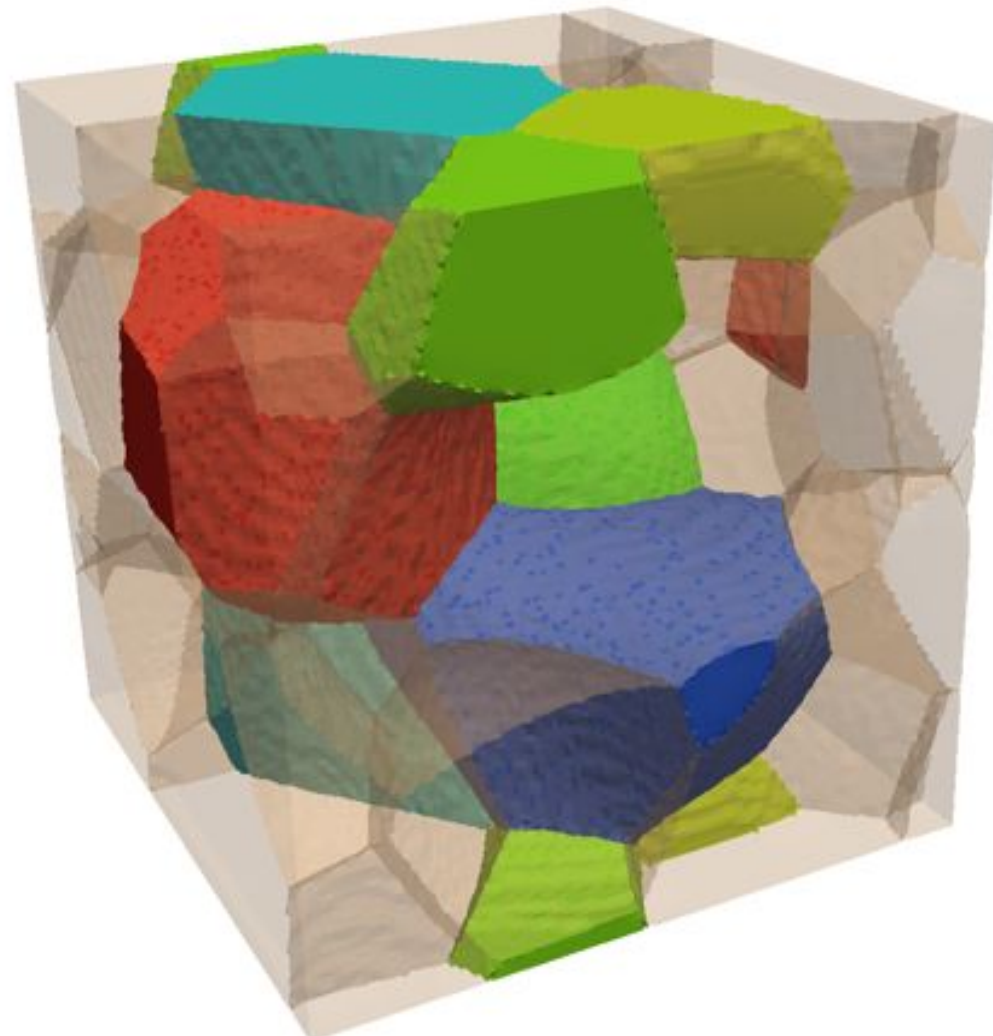
SCULPT Hexahedral Finite Element Mesh

SCULPT Interface Reconstruction



- Conformal grain boundary mesh
- Preserves grid in grain interiors
- Generates hexahedral elements

SCULPT Interface Reconstruction



Summary: Defects Beget Variability



- Voids in deformed Ta and welded 304L stainless steel
- Microstructure-induced uncertainty in metal deformation near defects
 - Holes in brass
 - Notches in Ta
 - Micro-springs
- Microstructure-scale mechanics in “large” components
- Stochastic reduced-order models for mechanical properties of partial-penetration 304L laser welds
- Conformal, hexahedral finite element meshing technology for three-dimensional polycrystalline microstructures